ACCSCIENCE PUBLISHING

Artificial Intelligence in Health

ORIGINAL RESEARCH ARTICLE

Discovery of new antibiotics using AI-guided spectroscopy and 3D drug-protein computer simulation technologies to combat MDR bacteria-associated mortality

Asit Kumar Chakraborty*, Meghna Maity, and Sumana Sahoo

Department of Biochemistry and Biotechnology, Faculty of Oriental Institute of Science and Technology, Vidyasagar University, Midnapore, West Bengal, India

Abstract

Multidrug-resistant (MDR), extensively drug-resistant (XDR), and totally drug-resistant bacteria can cause sepsis and death in patients due to their ability to inactivate most antibiotics, including ampicillin, tetracycline, streptomycin, chloramphenicol, erythromycin, and ciprofloxacin. This paper aims to review recent advancements in synthetic antibiotics, lantibiotics, and phytoantibiotics and to present our research on phytoantibiotics, specifically focusing on CU1 and NU2. While third- and fifth-generation synthetic antibiotics such as meropenem, moxifloxacin, amikacin, and tigecycline are currently relied upon for treating MDR infections, research is underway to develop peptide antibiotics known as lantibiotics (e.g., nisins, bacteriocins, and salivaricins). Lantibiotics such as nisin-A and salivaricin-B have demonstrated efficacy in curing numerous MDR infections, while phytochemicals such as artemisinin and quinine have shown effectiveness against chloroquine-resistant *Plasmodium falciparum* infections (malaria). In our study, we utilized techniques such as mass spectroscopy, nuclear magnetic resonance, and Fourier transform infrared spectroscopy in conjunction with artificial intelligence (AI) and computer simulation technologies to determine the structure of phytochemicals. Our results revealed that CU1, derived from *Cassia fistula* bark ethanol extract, exhibits potent antibiotic activity against XDR bacteria by targeting the RNA polymerases of *Escherichia coli* and *Mycobacterium tuberculosis*. Consequently, our MDR-Cure extract containing CU1 represents a promising antibacterial Ayurvedic medicine specifically tailored for skin and nail infections. Similarly, NU2 poly-fluorophosphate-glycosides from *Suregada multiflora* roots ethanol extract exhibited strong inhibitory effects on XDR bacteria by targeting DNA topoisomerase I. Recently, many cyclic peptide antibiotics have been synthesized *in vitro* using computer-guided AI technologies to predict 3D drug-enzyme interactions and are currently undergoing clinical trials. Our ultimate goal is to combat XDR bacteria-associated deaths, which are predicted to escalate as we approach 2050.

Keywords: Lantibiotics; Phytoantibiotics; Meropenem; Moxifloxacin; Salivaricin; Extensively drug-resistant tuberculosis

***Corresponding author:**
Asit Kumar Chakraborty
(chakraakc@gmail.com)

Citation: Chakraborty AK, Maity M, Sahoo S. Discovery of new antibiotics using AI-guided spectroscopy and 3D drug-protein computer simulation technologies to combat MDR bacteria-associated mortality. *Artif Intell Health.* 2024;1(2): 76-95.
doi: 10.36922/aih.2284

Received: November 21, 2023

Accepted: January 17, 2024

Published Online: April 23, 2024

1. Introduction

The penicillin antibiotic was discovered in 1928, leading to the development of numerous derivatives, such as ampicillin, amoxicillin, cefotaxime, imipenem, and meropenem, to combat bacterial infections.[1] Unfortunately, drug-resistance proteins in bacterial extracts were detected as early as 1940. It took 25 years to isolate the *amp* gene in pBR322 and to demonstrate that purified Amp penicillinase could cleave penicillin *in vitro*. Since then, drug companies have faced concerns that their new antibiotics might become obsolete within a few months of their commercial release. Modern multidrug-resistance (MDR) conjugative plasmids in bacteria are associated with mobile elements, integrons, integrases, transposases, and DNA topoisomerases, facilitating the emergence of new *mdr* genes that render newly developed antibiotics ineffective and economically unviable. Despite these challenges, scientists continued to develop new derivatives of penicillin (cephalosporins and carbapenems), aminoglycosides (amikacin), quinolones (moxifloxacin, lomofloxacin), and many others. On the other hand, bacteria have evolved to carry genotypes such as *blaTEM, blaCTX-M, blaOXA-58, blaKPC*, and *blaNDM*, which encode enzymes capable of inactivating all first- to fifth-generation PENEM antibiotics.[2] Similarly, at least 20 TET drug efflux derivatives have been sequenced, and these enzymes efflux tetracycline or its higher derivatives such as doxycycline, minocycline, and tigecycline. Chloramphenicol acetyltransferases (*cat* gene) were first discovered in the inactivation of chloramphenicol by acetylation, followed by the identification of AAC3' and AAC6' enzymes in bacterial plasmids responsible for acetylating streptomycin, amikacin, or erythromycin. The discovery of *StrA* and *StrB,* two linked genes in plasmids, has enhanced our understanding of how these two enzymes phosphorylate streptomycin to inactivate the tuberculosis (TB) drug. Lately, dozens of such isomers (APH2', APH3', and APH6') have been discovered to inactivate most amino-glycoside antibiotics.[3-5]

We also observe conventional point mutations in target enzymes, such as rpoB (RNA polymerase subunit) and gyrA/B (DNA topoisomerase II subunits), which lead to the inhibition of the binding of drugs rifampicin and ciprofloxacin, respectively, to the target enzyme, thereby preventing them from exerting their inhibitory effects. Consequently, the rate of approval for new antibiotic derivatives has decreased significantly, with only 2 – 5 approvals per year compared to hundreds released annually between 1970 and 2000 for commercial therapy of infectious diseases.[6,7]

Lantibiotics are cyclic peptide antibiotics produced by *Streptomyces, Streptococcus, Lactobacillus,* and other bacteria to combat other surrounding bacteria and microbes.[8,9] This diverse class includes gramicidins, salivaricins, mutacins, nisins, bacteriocins, and other lantibiotics, which hold promise for commercial use in combating MDR bacteria. Recombinant technology is now employed to express lantibiotic cyclase, lantibiotic synthetase, and lantibiotic transferase-peptidase to develop special types of cyclic peptide reactions, resulting in the development of novel trypsin-resistant peptide antibiotics against MDR bacteria. To avert MDR, it is imperative to avoid non-prescription and uncontrolled antibiotics and refrain from releasing antibiotics or lantibiotics into rivers, ponds, and seas.[10]

In ancient times, India and China were renowned for their rich tradition of herbal preparations to cure diverse diseases, including bacterial and fungal infections. However, during British rule, India's ancient tradition of herbal drugs waned, while China continued to prioritize herbal drugs.[11] Nevertheless, studies from the United States have demonstrated the efficacy of a phytodrug, artimisinin derivatives, to combat chloroquine-resistant malaria parasites, as well as the ability of phytodrugs, taxol, and topotecan to cure various types of cancer.[12] Despite India's daily publication of numerous papers on phytoextracts with antibacterial activities, commercialization has been hindered by the low bioactive chemical content and poor inhibitory power of such extracts.[13] We made our first important progress in isolating CU1 poly-bromophenol-turpentine from *Cassia fistula* bark targeting RNA polymerase.[14,15] Furthermore, we developed a large-quantity purification process of NU2 poly-fluorophosphate-glycosides from *Suregada multiflora* root using thin-layer chromatography (TLC) and ultraviolet (UV)-shadowing, targeting MDR bacterial DNA topoisomerase I (in preparation). NU2 has also exhibited an inhibitory role against the malaria parasite *Plasmodium falciparum* that resides in the human red blood cell.

Plant secondary metabolites are naturally produced compounds that can inhibit soil bacteria. MDR bacteria are known to proliferate in various environments, including soil, water (pond, river, sea, rain), chicken meat, milk, and human skin and hair. This constant exposure to newer strains of MDR bacteria suggests that plants may continuously produce new antibiotics, making plant extracts an ideal source for developing newer drugs against MDR bacteria and fungus. Our goal is to review the recent development and outcome of synthetic antibiotics, lantibiotics, and phytoantibiotics that are related to our phytodrug development program. However, we have carefully avoided the development of new synthetic antibiotics, as many important reviews are available.[16]

Instead, we emphasized on peptide antibiotics, which are novel in their preparation and mode of action.[17]

2. Materials and methods

2.1. PubMed and database search

We conducted a search on PubMed (www.ncbi.nlm.nih.gov/pubmed) using the following terms: "MDR bacteria," "nisin," "salivaricin," "phyto-drugs," "herbal drugs," and "MDR plasmids."

2.2. Isolation of multi-drug-resistant bacteria

We isolated MDR bacteria from samples obtained from the Ganges River by plating 0.1 mL of water onto LB+agar+50 µg/mL ampicillin or other antibiotics. Following incubation, single colonies were selected and tested for various drug sensitivities using different antibiotic-impregnated papers. Plasmids were isolated using the alkaline lysis method as described in Maniatis *et al.*[18] The polymerase chain reaction (PCR) was conducted using a standard PCR kit employing specific forward and reverse primers targeting *mdr* genes, including *bla, tet, acrA, mcr,* and *16s rRNA* genes for 30 cycles (95°C for 45 s, 52°C for 1 min, and 72°C for 1.5 min). The sequencing of PCR fragments was performed at Xcelris Labs Ltd., India. The primers used in this study are presented in Table 1.

2.3. Preparation of phytoextracts and purification of NU2 and CU1

Phytoextracts were prepared by adding 5 mL of ethanol to 1 g of semi-dry chopped root or bark in a 50 mL German-made plastic tube and left overnight at room temperature (25 – 30°C). Purification of NU2 and CU1 phytochemicals was carried out using preparative TLC (20 × 15 cm). The CU1 band was visually identified and cut, while the NU2 band was cut under UV illumination. Silica band was extracted with pure ethanol and centrifuged at 10,000 rpm for 10 min to obtain a clear solution which was then dried at room temperature.

2.4. Biochemical and molecular biological assays

The methyl red assay principle is based on mixed acid fermentation (acetic, lactic, and succinic) by certain bacteria, resulting in a significant pH decrease in the medium, dropping below 4.4. This pH change is indicated by a color change of the pH indicator, methyl red (2-dimethyl-4-amino azobenzene-O-carboxylic acid), turning from yellow when the pH is above 5.1 to red at pH 4.4.

The Voges-Proskauer assay, named after two pioneering microbiologists, is used to detect the formation of acetyl methyl carbinol by bacterial metabolism, a product of the butylene glycol pathway. Organisms such as members of the *Klebsiella-Enterobacter-Hafnia-Serratia* group produce acetoin as the chief end product of glucose metabolism and form smaller quantities of mixed acids. In the presence of atmospheric oxygen and 40% potassium hydroxide, acetoin is converted to diacetyl, which is then converted into a red complex under the catalytic action of alpha-naphthol.

Simmons citrate agar serves as an agar medium used for the differentiation of *Enterobacteriaceae* based on the utilization of citrate as the sole source of carbon. In the early 1920s, Koser developed a liquid medium formulation for the differentiation of fecal coliforms from the coliform group.[19] Simmons later modified this formulation to produce a solid medium that eliminated potential errors when interpreting growth. When the bacteria metabolize citrate, the ammonium salts are broken down to ammonia, which increases alkalinity. This shift in pH turns the bromthymol blue indicator in the medium from green to blue above pH 7.6.

Table 1. Primers used in this study[14]

Name	Sequence of the primers	Tm	Size
P27F	5'-AGA GTT TGA TCC GAA CGC T-3'	62°C	1.4 kb
P1392R	5'-TAC GGC TAC CTT GTT ACG ACT TCA-3'	65°C	
cmrF	5'-TTC GTT AGT CTG CCG TTG CT-3'	56°C	323 bp
cmrR	5'-ATC GCT GGC AAA CAG GGT TA-3'	57°C	
tem-sF1U	5'-ATGATGAGCACYTTTAAAGT-3' Y=C/T	56°C	312 bp
tem-sR1U	5'-TCATTCAGYTCCGKTTCCCA-3'Y=C/T; K=G/T	58°C	
tetF	5'-CTT CGC TAC TTG GAG CCA CT-3'	57°C	910 bp
tetR	5'-GCA GAC AAG GTA TAG GGC GG-3'	57°C	
acrAB-F	5'-ATG CTC TCA GGC AGC TTA GCC-3'	59°C	1 kb
acrAB-R	5'-TGT CAC CAG CCA CTT ATC GCC-3'	59°C	
ctxF1U	5'-AACACMGCMGATAATTCACA-3' M=A/C	59°C	586 bp

The urease assay is simple. Many organisms, especially those that infect the urinary tract, possess a urease enzyme capable of splitting urea in the presence of water to release ammonia and carbon dioxide, thereby increasing the alkalinity of the medium. This alkaline shift causes the indicator phenol red to change from its original orange-yellow color to bright pink.

2.5. High-performance liquid chromatography purification of CU1

The HPLC analysis was conducted at the CSIR-Indian Institute of Chemical Biology, Kolkata, and IIT-Mandi in Himachal Pradesh.[4,5] For the analysis, 5 mg of the TLC-purified active sample was dissolved in 0.5 mL of methanol. After filtration through a membrane filter, 0.1 mL of the sample was loaded onto an HPLC C-18 column pre-equilibrated with methanol.

2.6. Elementary analysis of CU1 and NU2

Elementary analysis was conducted at the Indian Association for the Advancement of Science (IAAS), Kolkata. A total of 4 mg of pure CU1 antibiotic was analyzed for its elemental composition using a Perkin Elmer Elementary Analyzer and compared with the standard. The obtained data included the percentage (%) of carbon and hydrogen. The percentage (%) of oxygen is calculated using Equation I:

$$\%O = 100\% - (\%C + \%H) \quad (I)$$

Our result revealed a notably high oxygen content in CU1 and NU2. In addition, we identified halogen in the structure, confirmed through mass spectroscopy, and further supported by nuclear magnetic resonance (NMR) spectra.

2.7. Mass spectroscopy of CU1

Mass spectroscopy was conducted at the Central Instrument Facility of Bose Institute and the Indian Institute of Science, India. A mass spectrum presents an intensity *versus* m/z (mass-to-charge ratio) plot (histogram), which is unique for each plant alkaloid. Typically, a pure chemical sample is bombarded by a laser, and the resulting positively charged particles are detected by a high-intensity magnet, separating molecular ions and their fragments using a mass spectrometer. This instrument comprises three main components: an ion source, a mass analyzer, and an artificial intelligence (AI)-guided detector. The common fragmentation processes for organic molecules are McLafferty rearrangement and alpha cleavage, which represent unique multiline graphs that aid in identifying a similar molecule and its derivatives. Lighter ions get deflected by the magnetic force more than heavier ions based on Newton's second law of motion, F = ma. In 1911, J. J. Thomson determined the ratio of electrical charge to the mass of an electron (e/m), which is 1811 times less than that of a hydrogen ion.[20] Francis W. Aston introduced the mass spectrograph[21] and won the Nobel Prize in 1922.

2.8. Fourier transform infrared spectroscopy (FTIR) of CU1

The FTIR spectroscopy was conducted at the Central Instrument Facility at Bost Institute, India. The infrared spectra provide information on the functional groups present in a compound. Wave number (v cm^{-1}) is used to measure the infrared absorption within the range of 4000 – 667 cm^{-1} (2.5 – 15 μ wavelength or λ), where v = E/hc and λ=1/v; c = velocity of light and h = Plank's constant. A nonlinear molecule consisting of n atoms has 3n-6 vibrational modes of stretching, rocking, scissoring, wagging, and twisting, offering information on the functional groups of the molecule. Bending vibrations occur at a lower wavenumber than stretching vibrations. Distinctive absorption bands are observed for different types of bonds: carbon triple bond absorption at 2300 – 2000 cm^{-1}; carbon double bond absorption at 1900 – 1500 cm^{-1}; and carbon single bond at 1300 – 800 cm^{-1}; O-H stretching absorption at 3570 cm^{-1}; C-H stretching at 3030 – 2860 cm^{-1}; C-H bending at approximately 1460 cm^{-1}; C=O stretching at approximately 1725 cm^{-1}; N-H stretching at 3500 cm^{-1}; N-H bending at approximately 1650 cm^{-1}; C-N stretching absorption at 1350 cm^{-1}; and C=N at approximately 2200 cm^{-1}. For the analysis, 5 mg HPLC-purified dry active chemical was mixed with 200 mg IR-grade KBr, and a tablet was prepared using a 13-mm die set (Kimaya Engineers, India) at a pressure of 10 kg/cm^2. Spectra were obtained using a Perkin Elmer Spectrum 100 FT-IR Spectrometer (serial no. 80944) for 10 min.[22]

2.9. Nuclear magnetic resonance spectroscopy of CU1

^{3}H-NMR and ^{13}C-NMR analyses were performed at IIT-Mandi, Himachal Pradesh, North India, and Bose Institute. Nuclear magnetic resonance is a spectroscopic technique employed to detect local magnetic moments around odd atomic nuclei when bombarded with radio waves. The most commonly used small molecules are hydrogen (^{1}H) and carbon (^{13}C) but ^{11}B, ^{19}F, ^{23}Na, ^{31}P, ^{35}Cl, etc. also been studied using NMR. At a low energy radio frequency, the nuclei magnetic spin quantum energy is represented by Equation II:

$$E = -\gamma m h B_0 \quad (II)$$

Where B_0 is the field strength, m = Magnetic spin quantum number, γ = Gyromagnetic ratio, and h is Plank's

quantum number. For data analysis, NMR absorption spectra were adjusted to the chemical shift (δ) using tetramethylsilane (TMS) as a standard, and the data were expressed as ppm (parts per million). Tetramethylsilane is chemically inert, magnetically isotropic, miscible with most organic solvents, and absorbs at a higher frequency compared to common types of organic protons. Equation III is used to calculate the δ:

$$\delta = \Delta v \times 10^6 / \text{oscillator frequency in cps} \quad \text{(III)}$$

Where Δv is the difference in magnetic spin absorption frequencies of the sample and the reference in cps (cps is approximately 700 cycles/s).

2.10. RNA polymerase assay

The RNA polymerase assay was conducted using 0.2 mM XTPs, 10 mM $MgCl_2$, 1 unit RNA of polymerase, 200 ng denatured CT-DNA, and 10 μci α-P^{32}-UTP. The reaction was carried out at 35°C for 15 min, after which it was spotted on diethylaminoethyl (DEAE) paper and washed with 0.5 M sodium phosphate, followed by ethanol. The dried paper was then counted on a scintillation counter. The RNA polymerase assay was performed at the Indian Institute of Science, specifically in Prof. Dipankar Chatterjee's laboratory. A more recent fluorometric RNA polymerase assay using plasmid DNA as a template was conducted at Bose Institute (Dr. Jayanta Mukhopadhyay's laboratory).[15]

3. Results and discussion

3.1. Mechanism of *mdr* genes' function and drug resistance

Figure 1 demonstrates the roles of early penicillinase and beta-lactamases (blaTEM, blaSHV, blaKPC, blaOXA, and blaNDM) in inactivating the penicillin drugs by cleaving the beta-lactam ring to produce penicillinic acid. Similarly, Figure 2 depicts the structure of streptomycin, with arrows indicating different sites on the drugs where AAC and APH-like drug-acetylating and drug-phosphorylating enzymes add a phosphate group or acetyl group to inactivate the drugs. The ANT enzymes also inactivate such drugs by adding an adenyl group to them. In Figure 3, we have presented the classification of different *mdr* genes and their emergence over time. This depiction underscores the rapid evolution of *mdr* genes in response to the introduction of a new antibiotic derivative, conferring upon bacteria the capability to neutralize new drugs. Nowadays, bacterial plasmids acquire DNA nikase, DNA topoisomerases, DNA integrases, transposes, and integrons in such a way that, when exposed to a new chemical, the bacteria begin to rearrange on plasmids to create a new *mdr* gene. Table 2 demonstrates the accumulation of *mdr* genes in both large and small bacterial plasmids. It includes an example of the generation of large plasmids that were sequenced and obtained from the NCBI GenBank Database (www.ncbi.nlm.nih.gov/nucleotide) by putting the accession number (Table 2). We downloaded the plasmid sequences and performed multi-alignment to see the percentage similarities among them because such different plasmids had many common *mdr* genes.[17]

It is challenging to develop a new *mdr* gene against a new antibiotic. However, in the expansive environment of soil, water, and the intestines of humans and animals, nature's laboratories surpass human research laboratories. This is because environmental bacteria are acquiring newer *mdr* genes via conjugation from MDR-bacterial plasmids at a rate of approximately a 5% increase per year. At present, the Ganges River water hosts 45 – 50% ampicillin-resistant bacteria, but the percentage of cefotaxime-resistant bacteria is much lower at 5%. However, imipenem-resistant bacteria are challenging to detect in Ganga River bacteria using conventional plating assays with 0.1 mL water on a 10 cm LB+agar+1 mg/mL imipenem plate. To isolate the imipenem-resistant bacteria, we added 5 μg/mL imipenem to 10 mL Ganges River water and 2 mL 6XLB medium and then incubated the mixture overnight at 37°C. Next, we serially diluted the overnight imipenem-resistant bacteria and plated them on 20 μg/mL imipenem to get single colonies. For simplicity, the total number of bacteria = 12200 cfu/mL, ampicillin-resistant bacteria = 5840 cfu/mL, cefotaxime-resistant bacteria = 50 cfu/mL, and imipenem-resistant

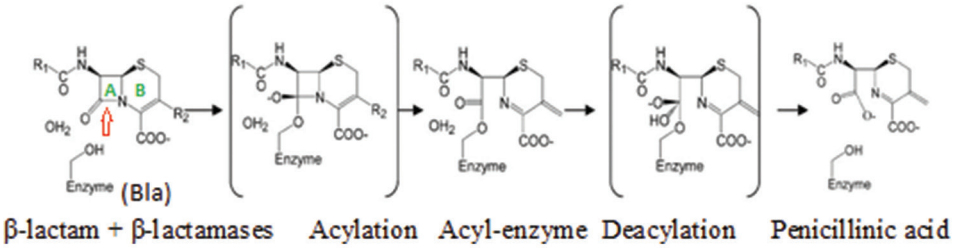

Figure 1. Inactivation of penicillin drugs by beta-lactamases (blaTEM, blaOXA, blaKPC, and blaNDM)

bacteria = 0.2 cfu/mL. Therefore, the chance of infection by imipenem-resistant bacteria is approximately 579 times lower than that of ampicillin-resistant bacteria by bathing or consuming Ganges River water. Thus, more people may be infected by ampicillin-resistant bacteria and still be cured with cefotaxime and imipenem drugs.

Certainly, in 2050, when the percentage of imipenem-resistant bacteria has increased, the situation will be different. It will be simpler to identify imipenem-resistant bacteria by plating 0.1 mL Ganges river water onto a 10 cm LB + agar + imipenem plate. In 2050, doctors are likely to perform drug sensitivity assays first using 100 antibiotic paper disks to determine the nature of a patient's blood, whether it is an MDR, extensively drug-resistant (XDR), or IDR infection. Obtaining such an assay result may cost a few thousand rupees, and one may have to wait for 2 days in order for the doctor to prescribe the correct antibiotic. One of the authors (Asit Kumar Chakraborty) shares a personal experience here. In 2022, the author contrasted an infection, and the doctor prescribed the cefotaxime drug, which was proven effective. However, to avoid the risk of MDR development, the author was subsequently prescribed two higher derivatives of tetracycline and aminoglycoside antibiotics. Fast forward to 2050, and a similar scenario may unfold differently. For instance, if the author were to bathe in the Ganges River, the initial cefotaxime treatment may not be effective, and if amikacin was also ineffective, then hospitalization would be recommended, usually accompanied by drug-sensitivity testing. In such cases, doripenem and meropenem therapy may be considered next, but if the totally drug-resistant (TDR) infection or if all 100 available antibiotics in Kolkata medical stores have failed, then the doctor would seek help from the USA to obtain expensive and high-risk investigational drugs. This is why scientists have predicted that there could be 10 million deaths in Asia annually by 2050. Simply put, people will not be able to afford the costly therapy, leading to their demise. In this paper, we have demonstrated the inactivation mechanism by diverged penicillinases (Figure 1) and have also demonstrated the acetylation, adenylation, and phosphorylation of different aminoglycosides acetyl-transferase (AAC), aminoglycoside adenyl-transferase (AAD), and aminoglycoside phosphotransferase (APH) enzymes (Figure 2). In addition, we have depicted the gradual discovery of new antibiotics with the subsequent generation of new *mdr* genes to inactivate these new antibiotics (Figure 3). This ongoing process has been occurring since 1970 until the present day, and doctors are becoming increasingly exhausted by the continuous development of new MDR bacteria.

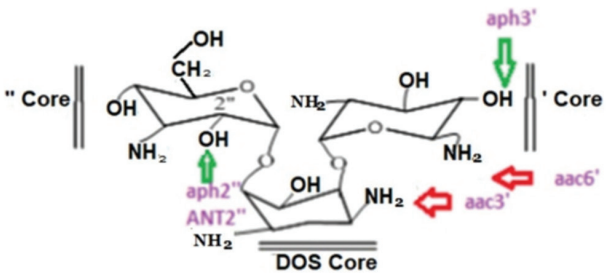

Figure 2. Inactivation of streptomycin by AAC, APH, and ANT MDR enzymes
Abbreviations: AAC: Acetyltransferases; APH: Phosphotransferases; ANT: Adenyltransferases; MDR: Multidrug-resistant.

In Figure 4, we presented the PCR assay results for the blaCTX-M1/2/9 genes using degenerative primers.

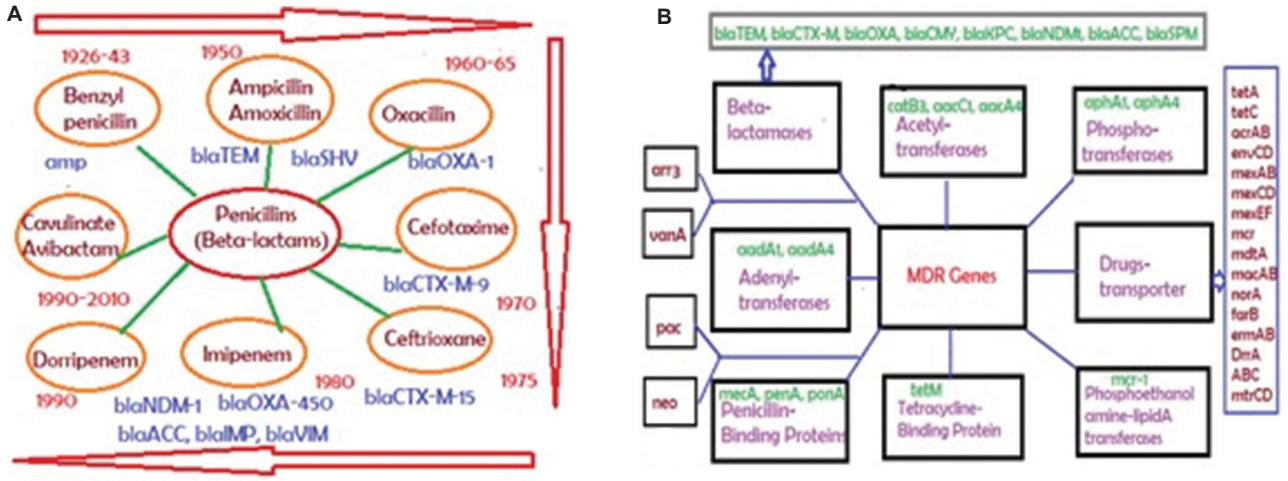

Figure 3. Drugs and MDR genes. (A) Gradual discovery of new penicillin drugs with time and the creation of new beta-lactamase derivatives. (B) Name of the different *mdr* genes and so many derivatives for beta-lactamases and the tetracycline membrane transporters, and other drug transporters (acrAB-TolC, mexAB-OprM, and macAB-TolC).

Table 2. Multidrug-resistant (*mdr*) genes in small and large plasmids

Accession number	Size (kb)	Multidrug-resistant marker genes: Drug transporters and antibiotic-inactivating enzymes	GenBank (year)	Pathogenic bacterial name
KC543497	501	blaOXA-10, MFS, blaTEM-8, ble, catB8, and aac3'	2014	*P. aerogenosa*
NC_018107	353	emrE, , crcB, NAT, terA/D, aph*, and blaTEM	2015	*K. oxytoca*
NC_022078	317	ABC, cat, aph*, aac3', cmr, tetA, and blaKPC	2015	*K. pneumoniae*
MG252895	300	FloR, tetA, StrB/A, sul2, blaCMY/OXA/NDM, aac6'-Ib, aphA7, arr2, cmlA1, aphA6, and sul1	2020	*E. coli*
LN555650	299	sul1, strA, catB, blaACC-1, aacA4, and blaVIM-1	2015	*S. enterica*
CP004000	295	bla$_S$HV-12, blaTEM-1, and ter C/A	2014	*K. pneumoniae*
CP007558	272	blaAmpC, ABC, sul1, blaTEM, aad, and ble	2014	*C. freundii*
JN420336	267	blaNDM1, blaOXA1, aac6', qnrB1, cat, and blaCTX-M,	2020	*K. pneumoniae*
NC_014312	251	blaKPC2, mph 2, ABC, blaAmpC, and qnrB	2014	*K. pneumoniae*
AP012055	250	blaNDM$_1$, aadA2, catA1, and qacA1	2013	*K. pneumoniae*
KM877269	249	aad, floR, hph, aac6'/3', , blaOXA-1, catB, arr3, and sul1	2015	*S. enterica*
CP011634	227	blaOXA, aad, blaTEM, aad, sul1, aac, and blaTEM	2015	*K. oxytoca*
HG530658	223	blaACC-1, strA, aadA2, aac3', rcnA, and pcoS	2015	*E. coli*
NC_019375	180	blaVIM, aacA7, dhfr, ANT3', SHV-5, sul1, and aph 3'	2014	*P. stuartii*
JX442976	172	tetA, aph, sul2, aadA1, blaOXA-10, Qnr, and blaCMY-16	2013	*K. pneumoniae*
NC_022522	168	blaCTX-M25, aacA4*, strB, strA, aadB, and blaOXA-21	2014	*S. enterica*
NC_012692	167	strA, blaCMY2, groEL, stbA, strB, flo^R, and merA	2014	*E. coli*
LN850163	167	MFS, AAA tetA, cat, blaTEM, macB, and blaCTX-M	2015	*E. coli*
NC_019121	166	blaAmpC, sul2, tetA, flo^R, hygB^R, and aph 3'	2014	*S. enterica*
LC055503	160	blaSHV12, aac6', blaOXA10, aadA1, sul1, and blaDHA1	2015	*K. pneumoniae*
FJ628167	151	blaKPC, sul1, qnrB4, blaDHA, mph 2, and ABC	2010	*K. pneumoniae*
JX182975	289	Cat, aadA2, sul1, ble, blaNDM1, dhfr, mph 2, and acrA/F	2020	*C. freundii*
KT185451	151	blaTEM/CTXM/SHV12, blaKPC, and blaNDM1	2015	*K. pneumoniae*
KF250428	151	blaIMP-4, aacA4, cmr, and flo^R	2013	*K. pneumoniae*
NC_012690	148	flo^R, tetA, strB, sul2, blaAmpC, sul1, aph, and blaTEM1,	2014	*E. coli*
AP012056	141	Aac3'/6', catB4, tetA, sul2, blaOXA/CTX-M, and strB/A	2013	*K. pneumoniae*
KF954760	140	blaTEM1, strA, strB, and aadA	2014	*K. pneumoniae*
KP893385	137	blaCTXM-65, blaKPC-2, blaSHV-12, and blaTEM-1b	2015	*K. pneumoniae*
HG941719	135	aadA5, mph, blaCTXM/OXA/TEM, aac6', sulI, and tetA	2014	*E. coli*
KF705205	134	hph, strA, aac3'-IV, tetA, and blaTEM-1	2015	*S. enterica*
NC_020087	133	aphA, hph, tetA, blaLAP$_2$, dhfr, ble, and qnrS1	2014	*K. pneumoniae*
CP009115	118	ble, blaOXA-1, qnr, and ble	2014	*K. pneumoniae*
GU256641	110	Sul2, strA, blaTEM1, blaSCO1, aacC2, and blaACC-4	2011	*E. coli*
NC_024978	110	dhfr, aad3, blaCTX$_1$, EtBr^R, and ABC-type	2014	*E. coli*
GU256641	110	Sul2, strA, blaTEM, blaSCO-1, aacC2, and blaACC-4	2011	*E. coli*
JX283456	108	blaKPC2, TolA, blaTEM, ABC transporter, and mph 2',	2012	*K. pneumoniae*
JX566770	107	pac, aadA1, dhfrA1, strB, and blaTEM-1	2013	*E. aerogenes*
MF042358	100	Aac3', ble, blaNDM-1, and sul1	2020	*E. cloacae*
CP009116	95	Aph, blaTEM, aac3', MFS, dhfr, aad, arr2, and blaNDM1	2014	*K. pneumoniae*
NC_019889	87	Aac (3')-II, blaNDM-1, sul1, MsrE, and mphE	2014	*K. pneumoniae*
KM406489	87	blaTEM-1	2015	*S. marcescens*

(Cont'd...)

Table 2. ***(Continued)***

Accession number	Size (kb)	Multidrug-resistant marker genes: Drug transporters and antibiotic-inactivating enzymes	GenBank (year)	Pathogenic bacterial name
GU585907	79	aadA2, aphA2, aadA1*, strA, strB, and blaVIM1	2010	*K. pneumoniae*
KF954759	73	blaKPC3, strB, aac (6'), and chrB	2014	*K. pneumoniae*
KJ460501	62	blaCTX-M	2014	*S. sonnei*
NZ_CP008901	52	Dhfr, blaKPC-2	2015	*E. cloacae*
AY046276	51	aadA1, blaOXA-2, sul1, tetA, and ABC	2012	*S. enterica*
KT225462	50	mphE, sul1, blaDHA-1, qbrB, strA, and strB	2015	*K. pneumoniae*
AB61665	47	blaIMP2, aacA4, aadA2, tetA, blaCTX-M, and sul1	2012	*K. pneumoniae*
KJ541071	44	sul1, blaOXA-2, aadA/B, blaTEM, catA1, and blaGES-5	2014	*E. coli*
JX104759	42	blaKPC-2 and ABC	2013	*K. pneumoniae*
KC354802	41	aacA4, aadA1, blaOXA-9, and blaTEM-1	2013	*K. pneumoniae*
NC_021087	26	blaGIM-1, aacA4, aadA1, blaOXA-2, and sul1	2015	*E. cloacae*
JN215524	24	Dhfr, cmlA, blaOXA10, aadA1, qnrB, blaDHA1, and sul1	2012	*C. freundii*
NG_035843	15	blaOXA-30, catB3, arr-3, sul1, qnr, and blaDHA-1	2014	*E. coli*
NG_041456	2.5	blaKPC-2	2014	*P. aeruginosa*
JN677524	1.9	Ble and blaNDM-1	2016	*K. pneumonia*

Abbreviations: *P. aeruginosa: Pseudomonas aeruginosa; K. oxytoca: Klebsiella oxytoca; K. pneumonia: Klebsiella pneumonia; E. coli: Escherichia coli; S. enterica: Salmonella enterica; C. freundii: Citrobacter freundii; P. stuartii: Providencia stuartii; E. aerogenes: Klebsiella aerogenes; E. cloacae: Enterobacter cloacae; S. marcescens: Serratia marcescens; S. sonnei: Shigella sonnei.*

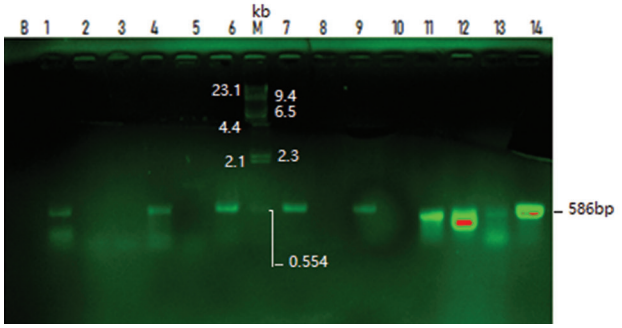

Figure 4. Detection of blaCTX-M1 genes in the Ganges River water MDR bacteria. Among 14 ampicillin- and tetracycline-resistant bacteria, five showed a clear, distinct band of 586 bp. The plasmid DNA was isolated from 6 mL bacteria (four 1.5 mL tubes) by the alkaline-lysis method following RNase A treatment, phenol-chloroform extraction, and ethanol precipitation
Notes: M = Lambda Hind-III marker; The primers are CTXF = 5'-AAC, ACM, GCM, GAT, AAT, TCA, CA-3' and CTXR = 5'-CCG, CRA, TAT, CRT, TGG, TGG, TG-3'

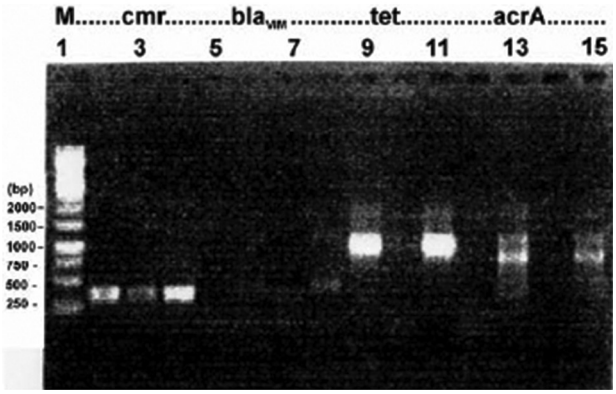

Figure 5. Localization of TET and ACRA drug efflux genes in *Escherichia coli* KT-1_mdr bacteria plasmids. We used both chromosomal DNA and plasmid DNA preparations, and it was prominent that both preparations had *tet* and *acrA* genes. The DNA was not CsCl gradient purified, and thus, due to large plasmids, such chromosome or plasmid classification was not possible. The blaVIM was not there (lanes 5 – 7), and cmr acetyltransferase must be there also (lanes 2 – 4)
Notes: Lane-1=100 bp DNA ladder as molecular weight marker, bla = 519 bp, tet = 910 bp, cmr = 323 bp, and acrA = 1007 bp.

The results revealed that 45% of MDR bacteria isolated from the Ganges River water subjected to ampicillin and tetracycline carried the blaCTX-M gene (586 bp band) in their plasmids. Similarly, the experiment conducted using blaTEM primers demonstrated that 100% of bacteria had the blaTEM gene in their plasmids (data not shown). In Figure 5, we further demonstrated that in MDR bacteria, the acrA and tetC drug efflux genes have been activated, indicating that MDR bacteria can remove multiple antibiotics from their cytoplasm, thereby increasing their MDR.[15]

We have also isolated MDR bacteria from chicken meat, milk, and human hair, which was found to be relatively easy. Plasmids were detected in these various antibiotic-selected MDR bacteria (Figure 6). We isolated 3 kb and 30 kb

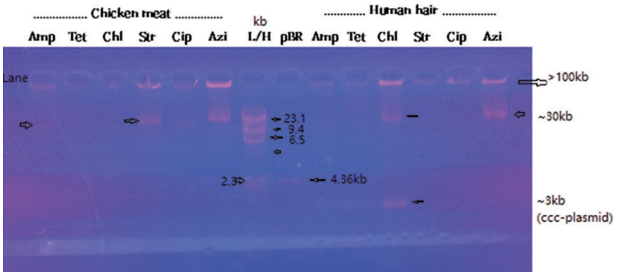

Figure 6. Detection of large plasmids and small plasmids in MDR bacteria selected with six old drugs. Plasmid DNA was isolated from 6 mL bacterial overnight culture and loaded onto 0.8% agarose gel and run for 4 h at 30 volts and ethidium bromide-stained (0.5 µg/mL in 1×TAE buffer). Lambda HindIII DNA and pBR322 plasmid DNA were used as markers. Six bacteria were isolated from a chicken meat sample (Midnapore city), and six other bacteria were isolated from human hair (salon in Kolkata city) and selected with six different antibiotic plates.

plasmids and then transfected them into the *Escherichia coli* DH5α laboratory strain that had no *mdr* gene and was highly sensitive to multiple antibiotics, either singly or in combination. We observed ampicillin resistance in the 3 kb plasmid, whereas there was no chloramphenicol resistance in the 30 kb plasmid, suggesting that the *cat* gene was located in larger plasmids (>200 kb), making it challenging to isolate using the conventional method from agarose gel at the Oriental Institute of Science and Technology (OIST) laboratory. Unfortunately, the plasmid contents in *E. coli* KT-1_mdr and *E. coli* KC-1_mdr were high and heterogeneous, resulting in a smear instead of distinct bands. Initially, we attributed this to contamination of our plasmid preparation with chromosomal DNA. Now, we understand that the MDR phenomenon is a mechanism of "genesis within" aimed at protecting bacteria in the intestine from the synthesis of 20 vitamins, which humans cannot produce on their own. Despite advancements, hunger persists, and the world population still does not have access to a balanced diet every day. In addition, many people, especially those from impoverished backgrounds, are reluctant to use multivitamin tablets. Consequently, we continue to depend on intestinal flora or probiotics. All creatures, including humans, depend on nature, and all habitats on Earth live symbiotically in different ways. Thus, it is important to conserve the environment and utilize phytoantibiotics, as proclaimed by the World Health Organization (WHO).

3.2. Isolation of chicken meat, milk, and human hair bacteria and their characterization

Our understanding suggests the presence of MDR bacteria in water, soil, and the intestinal tract. To investigate further, we collected human hair from a salon in South Kolkata, washed it with LB media, and plated it on LB-agar + ampicillin. Similarly, we obtained milk from a local vendor near the Midnapore station area and chicken meat from a local shop in Midnapore city. Antibiotic plates containing ampicillin, cefotaxime, tetracycline, streptomycin, ciprofloxacin, and erythromycin were selected for the analysis of all collected samples.

Next, we presented a few biochemical data supporting the heterogeneity of the MDR bacterial population in chicken meat and human hair. Figure 7 illustrates the results of the methyl red assay; Figure 8 demonstrates the results of Simmon's citrate utilization assay; Figure 9 depicts the urea test results; and Figure 10 demonstrates the sugar utilization test results to indicate the highly heterogeneous population of MDR bacteria. We utilized *E. coli* KT-1_mdr and *P. aeruginosa* DB-2_mdr as standards. The urea test yielded negative results for both MDR bacterial strains, while our selection of bacteria from the six antibiotic plates yielded few positive results. In addition, our 16S rRNA gene sequencing identified *Panalkaligenes* and *Stenotrophonomas* bacteria (Figure 11). However, due to our laboratory's lack of Biosafety Level 3 certification and the identification of potentially pathogenic MDR bacterial isolates in our data, we made the decision to suspend the project.

Recent research by Williams *et al.* involved sequencing the MDR bacterial population isolated from the stools of workers in poultry farms in Bangladesh. They compared the *mdr* genes with those found in poultry cecal and waste water resources.[23] They discovered many *mdr* genes, including *tetQ, blaTEM-1, blaSHV-1, and blaSHV-11*, in human fecal MDR bacteria. The other most abundant *mdr* genes are macrolide-lincosamide-streptogramin-resistant genes. In the poultry cecal samples, however, *SHV-27, blaSHV-110, blaOXA-65, and blaOXA-641*-like mdr genes were also located. In wastewater, the *blaOXA-58 mdr* gene, associated with MDR *Acinetobacter* bacteria, was found to be predominant, and such a protein could hydrolyze carbapenem drugs. The WHO has reported high contamination of poultry meat with CRE Enterobacteriaceae (*E. coli*), *Acinetobacter baumannii,* and *Pseudomonas aeruginosa* with isolated *mdr* genes showing homology to previously described plasmid sequences (accession numbers: CP058135, LC75731, CP054855, KY860573, and MN436715).[24,25]

3.3. Purification of abundant phytochemicals

Our extraction and purification procedures for active chemicals from the ethanol extract using TLC are straightforward, as demonstrated in Figures 12 and 13. We utilized eight 20×15 cm silica gel plates and processed 2.5 – 3 mL extract per TLC step in four tanks with lids. By employing repeated TLC, we were able to concentrate

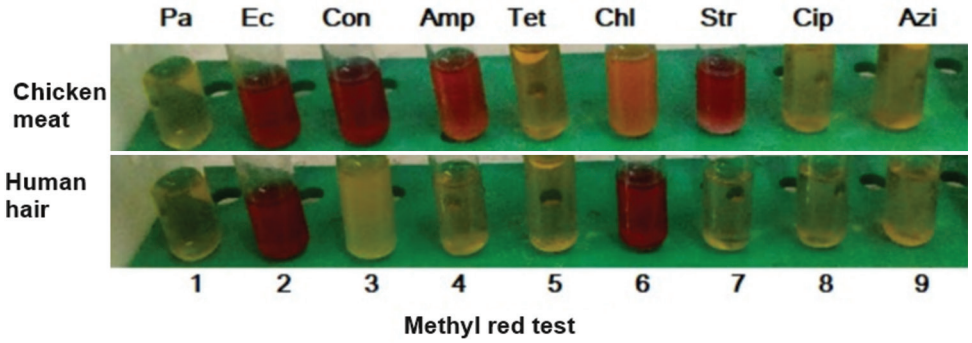

Figure 7. Methyl red assay of different drug-resistant bacteria isolated from chicken meat from Midnapore's meat shop and human hair from a local salon in Kolkata. Ampicillin-selected and streptomycin-selected chicken meat bacteria gave positive tests, whereas only chloramphenicol-selected human hair showed positive results, demonstrating the heterogeneity of the MDR bacterial population.
Abbreviations: Pa: *Pseudomonas aeruginosa* BD-2_mdr; Ec: *Escherichia coli* KT-1_mdr standard; Con: Control; Amp: Ampicillin; Tet: Tetracycline; Chl: Chloramphenicol; Str: Streptomycin; Cip: Ciprofloxacin; Azi: Azithromycin.

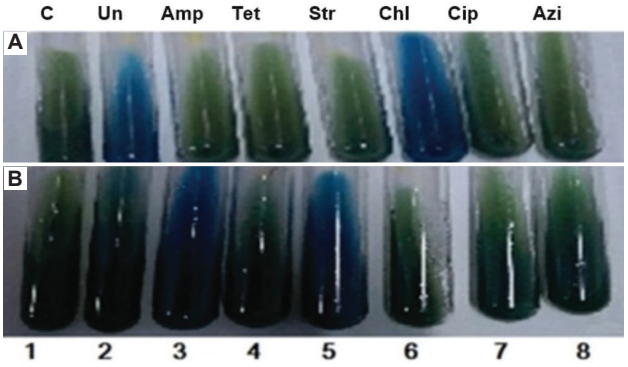

Figure 8. Simmon's citrate utilization test results. Chloramphenicol-selected chicken meat bacteria (A) gave a positive test, while both ampicillin-selected and streptomycin-selected human hair bacteria (B) gave a positive test result (blue color in LB + agar Simmon's citrate slant with bacteria).
Notes: C: Control tube, no bacteria added; Un: Un-selected and total bacteria without antibiotic; amp: Ampicillin; tet: Tetracycline (20 µg/mL); str: Streptomycin (50 µg/mL); chl: Chloramphenicol (25 µg/mL); cip: Ciprofloxacin (50 µg/mL); and azi: Azithromycin (50 µg/mL).

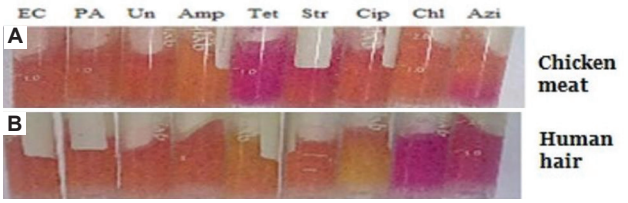

Figure 9. Urease test results. Both *Escherichia coli* and *Pseudomonas aeruginosa* did not yield a positive test. Tetracycline-selected chicken meat bacteria gave a positive result, and chloramphenicol-selected human hair bacteria also gave a positive result.

and purify CU1 and NU2 with 90 – 95% purity. Within a week, we collected a sufficient quantity of pure CU1 for biochemical analysis as well as for mass, NMR, and FTIR spectroscopic analyses. Figure 14 presents the potency of

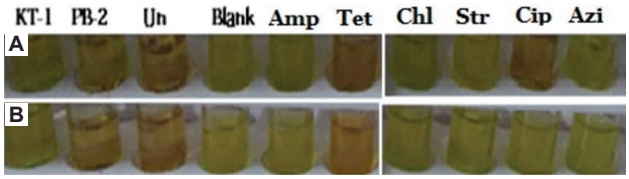

Figure 10. Sugar utilization test results. (A) chicken-derived bacteria and (B) human hair-derived bacteria. KT-1 is multidrug-resistance (MDR) *Escherichia coli,* and PB-2 is MDR *Pseudomonas aeruginosa*. Only tetracycline and ciprofloxacin-selected chicken meat bacteria gave a positive result, while only tetracycline-selected human hair bacteria gave a positive test result. Notes: Un means unselected bacteria; blank means reagent blank.

pure CU1, where ampicillin, ciprofloxacin, and ethanol had no effect on the growth of *E. coli* KT-1_mdr bacteria. In Figure 15, we describe the biochemical assays conducted to detect CU1, revealing that it is likely a turpentine polyphenol rather than a glycoside, anthraquinone, or alkaloid.

3.4. Computer-assisted AI-technology-guided modern spectroscopy technology for structure prediction of bio-active phytochemicals

In Figure 16, we presented the mass spectra showing a 75.5 mu line for bromine ion and DBr (82 mu) deviation high molecular weights bands for six bromine atoms. In Figure 17, we interpreted the FTIR spectra of CU1, whereby we observed a distinct band at 3000 – 3600 cm^{-1} indicative of the -OH group. In addition, peaks at 2960.1 and 2849.8 cm^{-1} signify $-CH_3$ stretching, while those at 1631.2, 1536.1, 1462.9, or 1387.9 cm^{-1}, suggest O-H bending, likely representing phenolics substituted with bromine atoms at a different position in the benzene ring. Furthermore, peaks at 1259.1 and 1134.0 cm^{-1} indicate C-C-C bending, while a peak at 719.8 cm^{-1} may represent $-CH_2$ rocking. Combining these findings

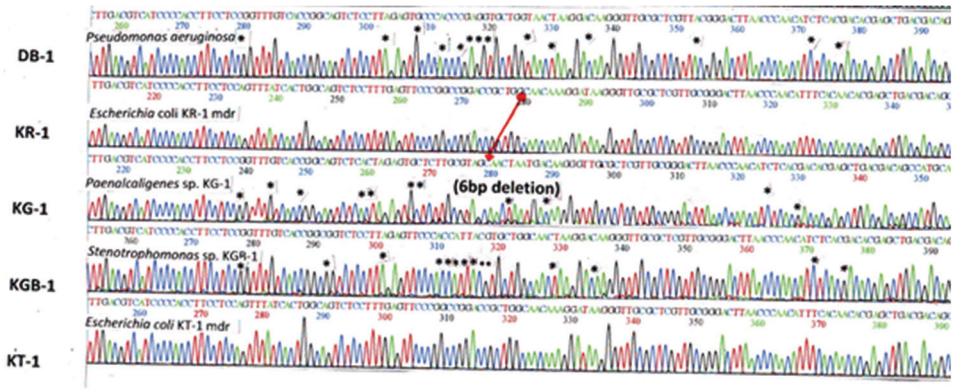

Figure 11. Sanger's DNA sequencing of the 16S rRNA gene of isolated multidrug-resistance bacteria from Ganges River water. Although the rRNA genes of different bacteria had high homology, we found differences among *Escherichia coli, Pseudomonas aeruginosa, Paenalkaligenes* sp., and *Stenotrophomonas* sp. The difference in position with the *E. coli* gene was indicated by black stars. The bacterial name was known from NCBI BLASTN (National Institutes of Health, USA) with derived sequences (not shown here).[14]

Figure 12. Ethanol extraction of *Cassia fistula* bark at room temperature overnight in German-made 50-mL plastic tubes. We avoided grinding the bark mechanically because that caused heating to inactivate the active chemicals CU1 and CU3 of *Cassia fistula* bark.

Figure 13. Preparative thin-layer chromatography (20 × 15 cm) of concentrated ethanol extract from *Cassia fistula* bark to isolate CU1 poly-bromo-phenol-saponins (dark band). The CU1 chemical is large but moves fast just below the solvent front (solvent: 40% methanol + 10% acetic acid + 50% water). Ethanol extract 300 – 400 µL was loaded onto each plate, giving a 0.5 cm broad band, dried at room temperature, and put onto 4 tanks with a lid, and ascending chromatography was done for 65 min.

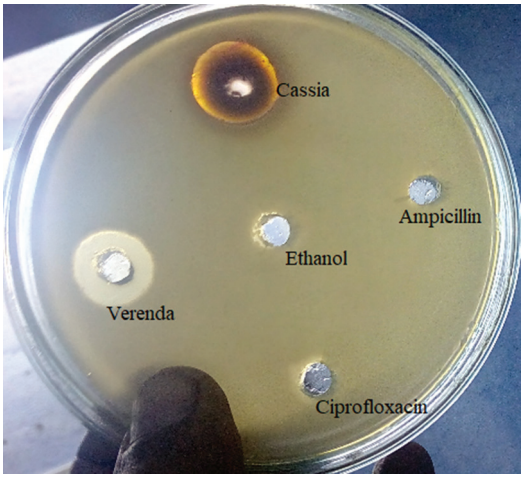

Figure 14. Agar hole assay of different 100% ethanol phytoextracts from *Cassia fistula* bark and *Jatropha gossypifolia* roots.

with elementary data analysis revealed that CU1 lacked nitrogen, and its carbon content was determined to be 35.9%, with hydrogen at approximately 5.5%. This data suggested that CU1 is a halogenated derivative, confirmed by the mass spectra. Further, carbon-NMR detected a C-Br bond at 23.7 ppm and a C-O bond, along with a polybenzoid compound at 165 ppm. Proton-NMR further suggested the presence of a polymeric phenol at ó 4.86 – 4.91 ppm with bromine substituents at ó 3.57 – 3.61 ppm (data not shown).[16]

3.5. Animal model and human clinical trial of CU1 MDR-Cure lotion

Next, we assessed the absorption of CU1 in rat intestines and its distribution into the bloodstream to cure *E. coli* KT-1_mdr infection. This treatment cured bacterial systemic infection, and the rats were alive for more

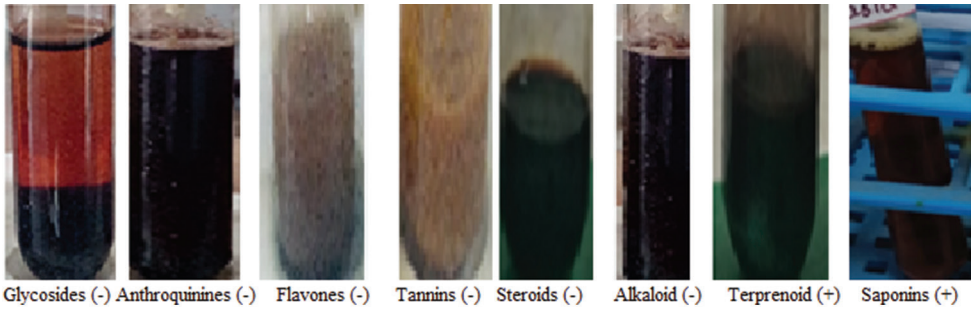

Figure 15. Phytochemicals assays for the thin layer chromatography-purified CU1 from *Cassia fistula* bark ethanol extract

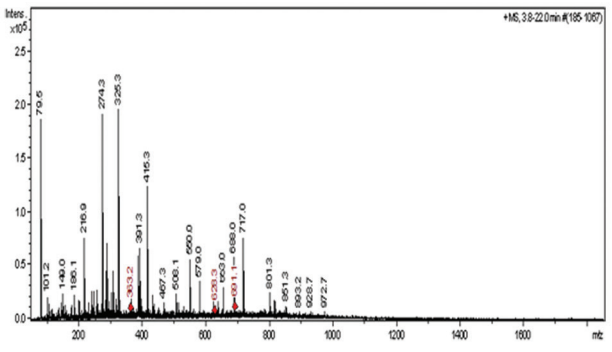

Figure 16. Mass-spectra of CU1 phytochemical. The results reveal a 79.5 mu band corresponding to the Br^- ion. The compound has a molecular weight above 927.7 mu.

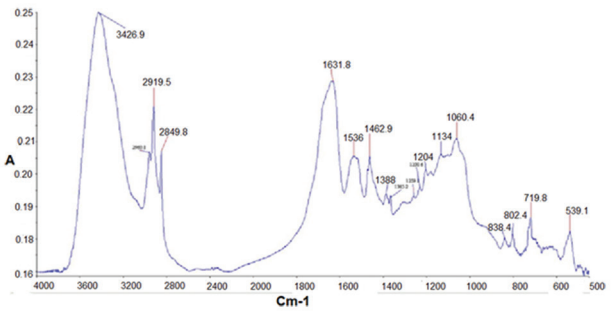

Figure 17. Detection of functional groups of the active compound CU1 by FTIR. The peak at 3426.9 is for N-H stretching and O-H stretching; 2960.1 and 2849.8 cm^{-1} are for CH_3 stretching; 1631.8 and 1536.1 cm^{-1} are for $CO\text{-}NH_2$ scissoring; 1462.9 and 1387.9 cm^{-1} represent O-H bending likely phenolics; 1259.1 and 11.34.0 cm^{-1} for C-C-C bending; and 719.8 may represent $-CH_2$ rocking.

than 3 months (Figure 18). We also treated human nail infection with both CU1 ethanol extract and MDR-Cure phytoextract, comprising neem bark and Haldi rhizome extract (50% ethanolic solution), chosen for their antioxidant and anti-inflammatory properties (Figure 19). Recently, we found that CU1 has no inflammatory effects, and it effectively cures human skin infections (data not shown). However, CU1 has no potential inhibitory effects on the growth of mammalian cells in culture,

Figure 18. Effectiveness of CU1 phytochemicals in rat animal model to clear *Escherichia coli* KT-1_mdr infection. Infection was induced by subcutaneous injection of 0.5 mL bacteria in five different locations on the skin. About 83% of bacterial load in tail-punctured blood was reduced by one oral dose (200 mg) of CU1 and not at all by 0.5 mL cefotaxime (200 mg).

Figure 19. Experiment on human nail chronic multidrug-resistant (MDR) infections. The infection was cured using MDR-Cure phytoextracts.

demonstrating its safety (data not shown). Similarly, we tested CU1 on the growth of molly fishes (red and black), and no significant inhibition of growth was observed, further suggesting the safety of CU1 drug for human use (data not shown).

3.6. Target identification of CU1 as RNA polymerase

We further investigated the molecular target of CU1 and identified its inhibition of *E. coli* RNA polymerase activity. Among the 11 phytochemicals tested, only CU1 exhibited inhibition comparable to the potent bacterial RNA polymerase inhibitor known as rifampicin.[16] As rifampicin is a potent anti-TB drug, we tested the efficacy of the CU1 drug on *Mycobacterium tuberculosis* RNA polymerase, revealing dose-dependent inhibition with increasing concentrations of CU1 (Figure 20).[16] However, in the DNA polymerase assay, there was no inhibition of *E. coli* DNA polymerase by CU1 (Figure 21). CU1 has no potential inhibitory effects on the growth of mammalian cells in culture, revealing that CU1 plays no role in human RNA polymerase activity (data not shown).

3.7. Lantibiotics research has gained momentum with AI-guided and computer-assisted 3D graphics of drug-enzyme interaction

The gramicidin peptide antibiotic has been long recognized to cure skin infections. It is produced by *Bacillus brevis*, which destroys gram-positive bacteria.[26,27] It disrupts bacterial membrane function and affects DNA and protein structure. Cyclic peptide antibiotics are good and more resistant to inactivation by MDR enzymes. Research is ongoing for the development of salivaricins, nisins, and related lantibiotics for combating XDR tuberculosis (XDR-TB). AI is important in understanding the 3D structural interaction between drugs and target proteins. Computer-assisted modification of drugs generated a good antibiotic with target specificity. For example, 3D crystal structure simulation clearly predicted the rifampicin drug's specificity for the *M. tuberculosis* RNA polymerases and was quite different from other similar RNA polymerases of *E. coli*, *S. aureus,* and *K. pneumoniae*. Thus, rifampicin is a first-line drug despite the emergence of *rpoB* gene (RNA polymerase beta-subunit) mutations that confer resistance. However, other TB-specific drugs such as

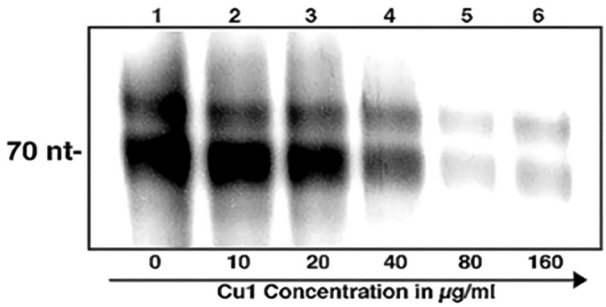

Figure 20. Run on transcription assay using *sinP* plasmid and *Mycobacterium* RNA polymerase. The RNA polymerase activity was gradually inhibited by increasing the concentration of CU1.[15]

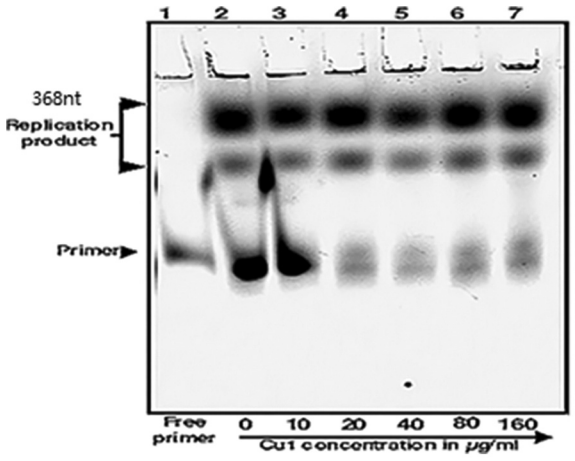

Figure 21. The *in vitro* DNA polymerase assay. The results demonstrate that increasing the concentration of CU1 has no effect on the enzyme.

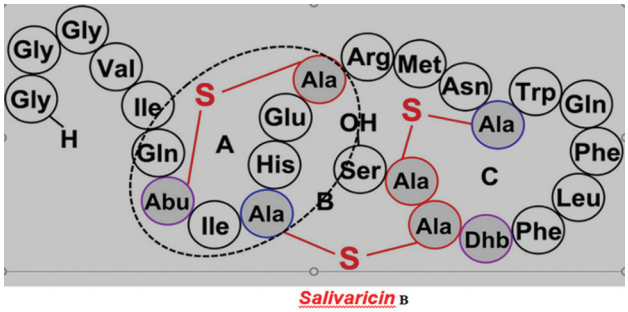

Figure 22. Complex cyclic structures of salivaricin-B lantibiotic that are effective against MDR bacteria. This peptide antibiotic was isolated from the oral bacteria *Streptococcus salivarious*, which contained many large plasmids with 10 salivaricin lantibiotic synthesizing genes.

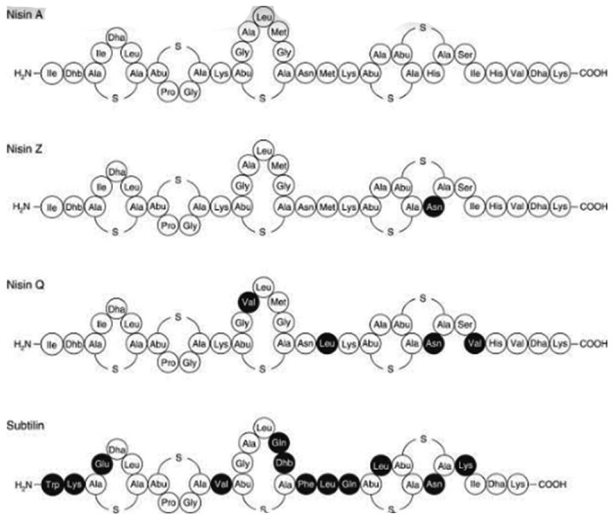

Figure 23. Structures of different isomers of nisin and subtilin lantibiotics. Such structural information was input into a computer device, and with the help of artificial intelligence technology, synthetic lantibiotics with a profound impact on extensively drug-resistant bacteria were formulated.

bedaquiline, ethambutol, pyrazinamide, and isoniazid are also prescribed. Therefore, it is crucial to develop more drugs that are resistant to all reported MDR enzymes, such as AMP, CAT, STR, BLA, AAC, APH, AAD, MCR, SUL, and DHFR.[15] The development of more specific TB drugs is essential due to the health risks associated with the current regimen, which entails orally ingesting 12 tablets. AI plays an important role in this endeavor. The mycolic acid complex in the outermost peptidoglycan layer of *M. tuberculosis* is unique to TB bacilli. Their 3D structure formulation is underway using computer graphics to design a more specific type of bedaquiline derivative, enough to kill TB bacilli within 3 – 7 days instead of months.[28,29] AI also aids in predicting easy absorption, blood transport, membrane transport, and target interaction with specificity, whereas 60 thousand cellular proteins would be unaffected. The TB situation in India has deteriorated to the point where it has more cases than any other 250 countries, with 27 million infections in 2022, despite the successful implementation of the directly observed therapy short course (DOTS) program.[7] Modern technologies such as NMR and FTIR, coupled with AI and computer simulation, aid in identifying the correct structure of new drugs, advancing TB treatment efforts.

Using AI technology, many peptide condensation and modification enzymes were cloned into plasmids, overexpressed, and purified. Scientists are developing new cyclic peptide antibiotics *in vitro* by utilizing such enzymes, which are then assayed for their effects on the XDR and TDR clinically isolated bacterial populations.[30] However, this task is challenging and requires increased funding. Unfortunately, these new drugs are likely to be costly, making them inaccessible to people in India as well as in African and Latin American countries due to their financial limitations.[31-33]

In Figures 22 and 23**,** we present the structures of salivaricin B and different nisin lantibiotics. Numerous publications in PubMed highlight the potential use of AI technology and computer software, along with 3D simulation, to develop newer lantibiotics against MDR bacteria.[34-45] In Figure 24**,** we demonstrate the multi-alignment of different lantipeptides that were heterogeneous and strongly diverse, derived from different bacterial origins. However, some similarities were observed in the salivaricins and nisins (Figure 23). In Figure 25**,** we identified a striking similarity between a mutacin and an unidentified protein located in the small plasmid pUA140 of *Streptococcus mutans*, a notorious carcinogen of the oral cavity and teeth. Figures 26 and 27 demonstrate the similarity of peptide condensing and peptide cyclase enzymes between *Streptococcus salivarious* and *Lactobacillus lactis*, both resident oral cavity bacteria. The similarity was almost 50%, and the sequences of those enzymes were well-conserved. Thus, genetic manipulation

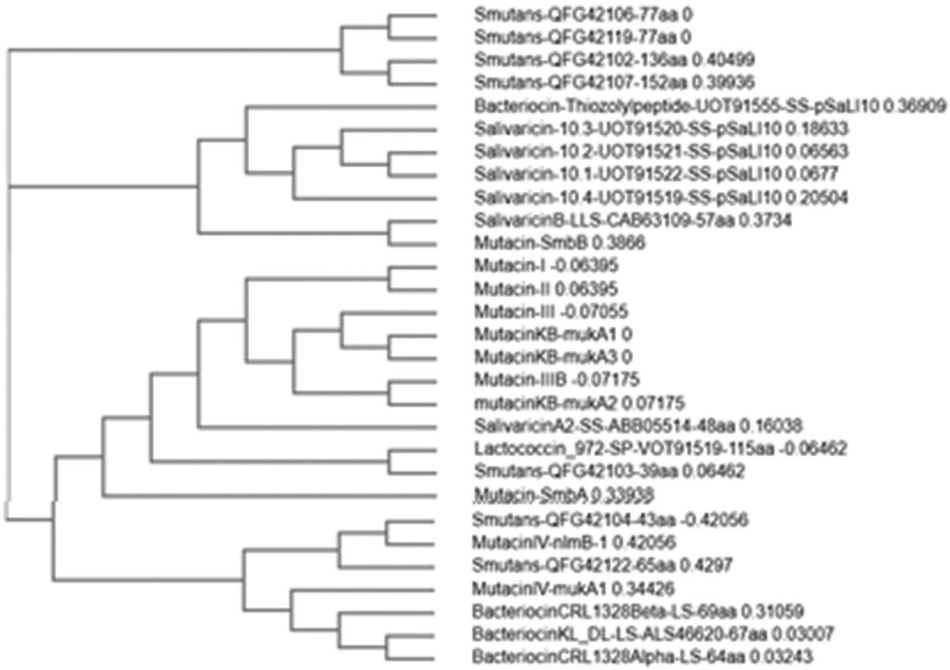

Figure 24. Phylogenetic analysis of different lantibiotics, such as salivaricins, mutacins, and bacteriocins, with broad range activities against multidrug-resistant bacteria

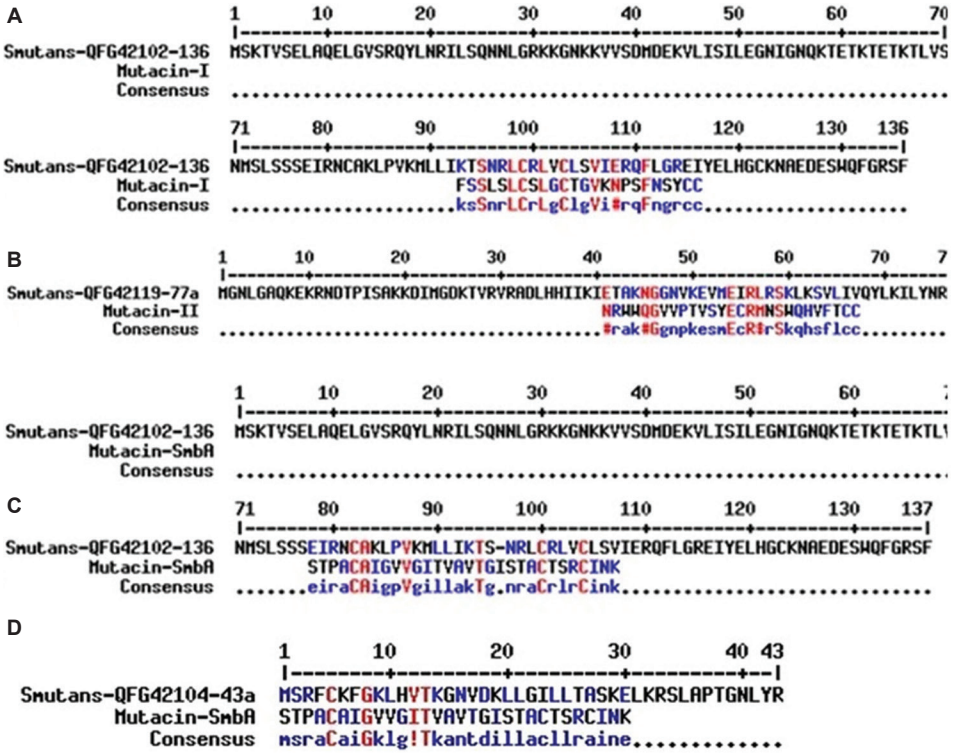

Figure 25. Demonstration of mutacins homology, a pre-lantibiotic protein within the *Streptococcus mutans* plasmid (pUA140). This bacterium, notorious for causing dental caries and oral cancer, utilizes lantibiotic to kill beneficial *Lactobacillus* bacteria. (A) Mutacin-I (strong homology); (B) Mutacin-II; (C) Mutacin-SnbA; (D) another Mutacin-SnbA.

Figure 26. Relationship between lantibiotic genes in oral bacteria, with 50% homology observed between *Streptococcus salivarius* and *Lactobacillus lactis*. These enzymes are cloned, overexpressed, and utilized to develop cyclic peptide antibiotics *in vitro*. The medical AI technology is employed to formulate unique salivaricin and lacticin-like antibiotics targeting membrane structures, inducing leakage of nutrients and subsequent death of extensively drug-resistant bacteria.

of these enzymes may lead to novel enzyme activity for the development of novel lantibiotics against XDR-TB.[30]

India has the highest burden of TB, with one in every 550 people at risk of *M. tuberculosis* infection. We trust in herbal drugs and the ancient Indian herbal drug prescription, as documented in Sanskrit books such as the Charaka Samhita, Susruta Samhita, and Atharva Veda, dating back 3000 years.[46,47] However, phytochemical purification

lanthionine synthetase LanC family protein [Lactococcus cremoris]	Lactococcus cremoris	465	465	56%	2e-161	95.42%	253	WP_308781485.1
lanthionine synthetase LanC family protein [Lactococcus]	Lactococcus	464	464	56%	2e-161	95.42%	252	WP_257788761.1
Nisin biosynthesis protein NisC [Lactococcus cremoris]	Lactococcus cremoris	461	461	54%	2e-160	99.56%	227	MDA2881859.1
nisin cyclase NisC, C-terminus [Lactococcus lactis]	Lactococcus lactis	459	459	54%	9e-160	99.56%	226	ANU04785.1
lanthionine synthetase C family protein [Streptococcus]	Streptococcus	454	454	97%	1e-154	52.83%	406	WP_038675133.1
putative lantibiotic cyclase SlvC [Streptococcus salivarius]	Streptococcus salivarius	452	452	97%	4e-154	52.83%	406	AEX55161.1
Nisin biosynthesis protein [Lactococcus lactis subsp. lactis NCDO 2118]	Lactococcus lactis subsp. l...	446	446	60%	4e-154	91.70%	253	AII12750.1
lanthionine synthetase C family protein [Streptococcus sp.]	Streptococcus sp.	451	451	97%	1e-153	52.58%	406	WP_293927884.1
lanthionine synthetase C family protein [Streptococcus]	Streptococcus	449	449	95%	5e-153	52.87%	406	WP_175063856.1
lanthionine synthetase C family protein [Ligilactobacillus salivarius]	Ligilactobacillus salivarius	382	382	97%	1e-126	50.36%	406	WP_117641665.1
lanthionine synthetase C family protein [Ligilactobacillus salivarius]	Ligilactobacillus salivarius	382	382	97%	1e-126	50.36%	406	WP_223688807.1
lanthionine synthetase C family protein [Ligilactobacillus salivarius]	Ligilactobacillus salivarius	382	382	97%	1e-126	50.36%	406	WP_160995820.1
lanthionine synthetase C family protein [Ligilactobacillus salivarius]	Ligilactobacillus salivarius	382	382	97%	2e-126	50.36%	406	WP_160995036.1
hypothetical protein B6U42_09335 [Ligilactobacillus salivarius]	Ligilactobacillus salivarius	381	381	97%	3e-126	50.36%	403	OQR12675.1
lanthionine synthetase C family protein [Ligilactobacillus salivarius]	Ligilactobacillus salivarius	381	381	97%	5e-126	50.36%	406	WP_160998371.1
lanthionine synthetase C family protein [Ligilactobacillus salivarius]	Ligilactobacillus salivarius	380	380	97%	7e-126	50.12%	406	WP_270354997.1

Figure 27. LanC/NisC/SlvC peptide cyclase proteins exhibit 50% homology across oral bacteria. There are many isomers of nisin lantibiotic produced by *Streptococcus lactis*: nisin-A, nisin-Z, nisin-Q, and nisin-U2. Nisin-H was isolated from *Streptococcus hyointestnalis,* and nisin-P from *Streptococcus gallolyticus.* Nisin-O was isolated from a gut bacteria called *Blautia obeum* A2-162. Nisin-J was produced by a Staphylococcus species, and nisin-G was produced by fecal bacteria such as *Streptococcus uberis* and *Streptococcus sius.*[52]

methods were not developed then, resulting in suboptimal doses. At present, we are developing phytodrugs (CU1 and NU2) from a few medicinal plants against MDR bacteria, following a few basic points. The phytochemicals must be present in sufficient amounts, typically constituting 30% of the ethanol extract of bark, root, or leaves. Their potency must be demonstrated by a 15 mm-diameter lysis zone or higher in the LB-agar bacterial lysis zone assay using a 1:5 ratio (plant parts: solvent) for overnight extraction at room temperature in a tightly capped plastic tube or bottle. Furthermore, these chemicals must be easily separated by preparative TLC and detectable either by the naked eye or the UV-shadow technique. Such phytochemicals must be cytocidal to at least ten MDR bacteria, initially selected with ten different antibiotics, and be resistant to at least six antibiotics, such as ampicillin, amoxicillin, cefotaxime, tetracycline, amikacin, linezolid, ciprofloxacin, novobiocin, trimoxazole, imipenem, streptomycin, chloramphenicol, erythromycin, azithromycin, lomofloxacin, norfloxacin, and tigecycline.[14,15]

Figure 28 outlines future strategies, emphasizing the potential for automation in drug discovery to revolutionize the development of new antibiotics. In other words, with the help of AI methods, we can outsmart XDR bacteria, which possess a myriad of *mdr* genes and transposons. Together with a slow and expensive antibiotic development pipeline, the proliferation of drug-resistant bacteria drives urgent interest in computational methods that promise to expedite candidate drug discovery.[45,48] Given the urgency of the antimicrobial resistance crisis, we must embrace open science best practices in AI-driven antibiotic discovery to accelerate preclinical research on potent new drugs.[49-53] Ultimately, AI-driven enhancements in drug discovery offer many opportunities

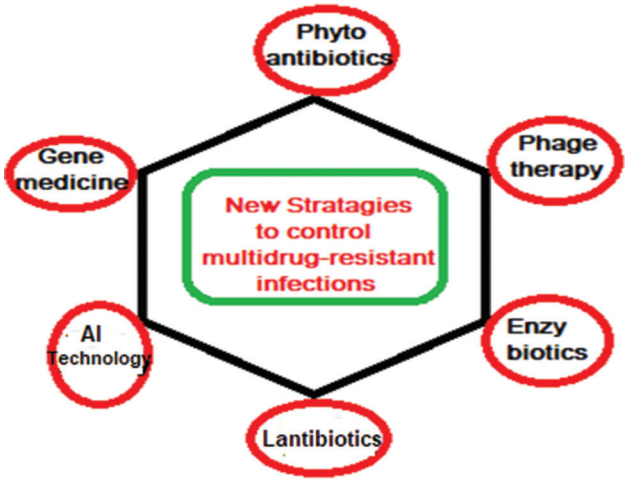

Figure 28. New research dimensions with the help of artificial intelligence technology to control extensively drug resistant and totally drug-resistant bacterial infections as we approach 2050

for future applications in antibiotic development against superbugs.[54-61]

4. Conclusion

The chemical synthesis of antibiotics remains vital, but it has faced challenges in recent times due to high costs and concerns over MDR. Nevertheless, extensive research on novel lantibiotics against XDR bacteria has been reported, positioning peptide antibiotics to take center stage in the coming years. Our research on phytoantibiotics (CU1 and NU2) has gained momentum, with the United Nations recognizing the promising global benefits of such work across all age groups. Our MDR-Cure extract represents a promising antibacterial ayurvedic medicine specifically tailored for skin and nail infections. In addition, while phage

therapy has emerged as a potential solution for bacterial infections, our attempts to cultivate a bacteriophage from the drain in Kolkata have been unsuccessful. The use of antibiotics, as well as gene medicine such as antisense and ribozyme, coupled with nanotechnology and AI, maybe a future strategy to combat MDR bacteria. Early intervention is key to averting a projected 10 million deaths by 2050 in Asian, African, and Latin American countries.

Acknowledgments

I am grateful to Dr. Ginger Iv for encouraging me to write this article. This article contains new data on MDR bacteria characterization and novel findings on the NU2 drug, which have been set aside due to patent application. As a retired professor of Biochemistry from Vidyasagar University, I had the privilege of collaborating with Meghna Maity and Sumana Sahoo on their MSc Biochemistry dissertations, which focused on characterizing MDR bacteria from chicken meat and human hair. I am also thankful to Dr. Jayanta Mukhopadhyay of Bost Institute, Kolkata, for his help in the article writing.

Funding

None.

Conflict of interest

The authors declare that they have no competing interests.

Author contributions

Conceptualization: Asit Kumar Chakraborty
Formal analysis: Asit Kumar Chakraborty
Investigation: Meghna Maity, Sumana Sahoo
Methodology: Meghna Maity, Sumana Sahoo
Writing – original draft: Asit Kumar Chakraborty
Writing – review & editing: Asit Kumar Chakraborty

Ethics approval and consent to participate

The animal experiment was approved by the Institutional Ethics Committee of Vidyasagar University .

Consent for publication

Asit Kumar Chakraborty gave consent to publish his data in this study.

Availability of data

Data used in this work is available from the corresponding author upon reasonable request.

Further disclosure

Asit Kumar Chakraborty gave online lectures on phytodrugs against MDR-bacteria aspect in Pharmaceutical Congress, Aver Conference, Tokyo on March 20, 2023; Clinical Microbiology conference, London dated March 21, 2023; Biotechnology conference, Rome on June 14, 2023, Pharmaceutical conference, Valencia, Spain on September 14, 2023, and Natural Medicine congress, Chicago, USA on October 11, 2023. A related review and research article by Asit Kumar Chakraborty relating MDR-TB was deposited to BioRxiv preprint (Doi: https://doi.org/10.1101/2023.09.04.556143 and https://www.biorxiv.org/content/10.1101/2020.11.04.369058v1). Most of the data were published in new open-access journals between 2015 and 2023.

References

1. McArthur AG, Waglechner N, Nizam F, *et al*. The comprehensive antibiotic resistance database. *Antimicrob Agents Chemother*. 2013;57(7):3348-3357.

   doi: 10.1128/AAC.00419-13

2. Woappi Y, Gabani P, Singh A, Singh OV. Antibiotrophs: The complexity of antibiotic-subsisting and antibiotic-resistant microorganisms. *Crit Rev Microbiol*. 2016;42(1):17-30.

   doi: 10.3109/1040841X.2013.875982

3. Das B, Verma J, Kumar P, Ghosh A, Ramamurthy T. Antibiotic resistance in *Vibrio cholerae*: Understanding the ecology of resistance genes and mechanisms. *Vaccine*. 2020;38(Suppl 1):A83-A92.

   doi: 10.1016/j.vaccine.2019.06.031

4. Chakraborty AK. High mode contamination of multi-drug resistant bacteria in Kolkata: Mechanism of gene activation and remedy by heterogeneous phyto-antibiotics. *Indian J Biotechnol*. 2015;14:149-159.

5. Chakraborty AK. Ganga action plan, heterogeneous phyto-antibiotics and phage therapy are the best hope for India tackling superbug spread and control. *Indian J Biol Sci*. 2017;23:34-51.

6. Moo CL, Yang SK, Yusoff K, *et al*. Mechanisms of Antimicrobial Resistance (AMR) and alternative approaches to overcome AMR. *Curr Drug Discov Technol*. 2020;17(4):430-447.

   doi: 10.2174/1570163816666190304122219

7. Chakraborty AK. Current status and unusual mechanism of multiresistance in *Mycobacterium tuberculosis*. *J Health Med Inform*. 2019;10(1):328.

   doi: 10.4172/2157-7420.1000328

8. Barbour A, Tagg J, Abou-Zied O, Philip K. New insights into the mode of action of the lantibiotic salivaricin B. *Sci Rep*. 2016;6:31749.

   doi: 10.1038/srep31749

9. Barbour A, Wescombe PA, Simtj L. Evolution of lantibiotic salivaricins: New weapons to fight infectious diseases.

Trends Microbiol. 2020;28(7):578-593.

doi: 10.1016/j.tim.2020.03.001

10. Miklasińska-Majdanik M. Mechanisms of resistance to macrolide antibiotics among *Staphylococcus aureus*. *Antibiotics* (*Basel*). 2021;10(11):1406.

doi: 10.3390/antibiotics10111406

11. Cowan MM. Plant products as antimicrobial agents. *Clin Microbiol Rev*. 1999;12:564-582.

doi: 10.1128/CMR.12.4.564

12. Ren Y, Yu J, Kinghorn AD. Development of anticancer agents from plant-derived sesquiterpene lactones. *Curr Med Chem*. 2016;23(23):2397-2420.

doi: 10.2174/0929867323666160510123255

13. Daglia M. Polyphenols as antimicrobial agents. *Curr Opin Biotechnol*. 2011;23:174-181.

doi: 10.1016/j.copbio.2011.08.007

14. Chakraborty AK. Multi-drug resistant bacteria from Kolkata Ganga River with heterogeneous MDR genes have four hallmarks of cancer cells but could be controlled by organic phyto-extracts. *Biochem Biotechnol Res*. 2017;5(1):11-23.

15. Chakraborty AK, Saha S, Poria K, Samanta T, Gautam S, Mukhopadhyay J. A saponin-polybromophenol antibiotic (CU_1) from *Cassia fistula* bark against multi-drug resistant bacteria targeting RNA polymerase. *Curr Res Pharmacol Drug Discov*. 2022;3:100090.

doi: 10.1016/j.crphar.2022.100090

16. Liu K, Huigens RW 3rd. Instructive advances in chemical microbiology inspired by nature's diverse inventory of molecules. *ACS Infect Dis*. 2020;6(4):541-562.

doi: 10.1021/acsinfecdis.9b00413

17. Tan HM, Lall AC, Keppo J, Chen SL. Evaluation of a new antiresistic strategy to manage antibiotic resistance. *J Glob Antimicrob Resist*. 2023;33:368-375.

doi: 10.1016/j.jgar.2023.03.006

18. Maniatis T, Fritsch EF, Sambrook J. *Molecular Cloning-A Laboratory Manual*. Cold Spring Harbor, NY, USA: Cold Spring Harbor Laboratory Press; 1982.

19. Koser SA. Correlation of Citrate utilization by members of the colon-aerogenes group with other differential characteristics and with habitat. *J Bacterol*. 1924;9:59-77.

doi: 10.1128/jb.9.1.59-77.1924

20. Thomson JJ. Cathode rays. *Philos Mag*. 1897;44(269):293-316.

doi: 10.1080/14786449708621070

21. Aston FW. LXXIV. A positive ray spectrograph. In: *The London, Edinburgh, and Dublin Philosophical Magazine and Journal of Science*. Vol. 38. United States: Creative Media Partners, LLC; 1919. p. 707-714.

doi: 10.1080/14786441208636004

22. Song Y, Cong Y, Wang B, Zhang N. Applications of Fourier transform infrared spectroscopy to pharmaceutical preparations. *Expert Opin Drug Deliv*. 2020;17(4):551-571.

doi: 10.1080/17425247.2020.1737671

23. Willams AD, Rousham E, Neal AL, *et al*. Impact of contrasting poultry exposures on human, poultry, and wastewater antibiotic resistomes in Bangladesh. *Microbiol Spectr*. 2023;11:e01763-23.

doi: 10.1128/spectrum.01763-23

24. Carvalho I, Chenouf NS, Carvalho JA, *et al*. Multidrug-resistant *Klebsiella pneumoniae* harboring extended spectrum β-lactamase encoding genes isolated from human septicemias. *PLoS One*. 2021;16(5):e0250525.

doi: 10.1371/journal.pone.0250525

25. Guclu AU, Gozen AG. Genetic diversity of OXA-like genes in multidrug-resistant *Acinetobacter baumannii* strains from ICUs. *Clin Lab*. 2020;66(10):20215-2019.

doi: 10.7754/Clin.Lab.2020.200135

26. Hotchkiss RD, Dubos RJ. Fractionation of the bactericidal agent from cultures of a soil *Bacillus*. *J Biol Chem*. 1940;132:791-792.

27. Ganz T. Defensins: Antimicrobial peptides of innate immunity. *Nat Rev Immunol*. 2003;3:710-720.

doi: 10.1038/nri1180

28. Imran M, Abida, Alotaibi NM, *et al*. Computer-assisted discovery of safe and effective DprE1/aaRSs inhibitors against TB utilizing drug repurposing approach. *J Infect Public Health*. 2023;16(4):554-572.

doi: 10.1016/j.jiph.2023.02.005

29. Taira J, Nagano T, Kitamura M, Yamaguchi M, Sakamoto H, Aoki S. Structural modification of a novel inhibitor for mycobacterium enoyl-acyl carrier protein reductase assisted by *in silico* structure-based drug screening. *Int J Mycobacteriol*. 2020;9(1):12-17.

doi: 10.4103/ijmy.ijmy_184_19

30. Wayah SB, Philip K. Purification, characterization, mode of action, and enhanced production of salivaricin MMAYE1, a novel bacteriocin from *Lactobacillus salivarius* SPW1 of human gut origin. *Electron J Biotechnol*. 2018;35:39-47.

doi: 10.1016/j.ejbt.2018.08.003

31. Foreman KJ, Marquez N, Dolgert A, *et al*. Forecasting life expectancy, years of life lost, and all-cause and cause-specific mortality for 250 causes of death: Reference and alternative scenarios for 2016-40 for 195 countries and territories. *Lancet*. 2018;392(10159):2052-2090.

doi: 10.1016/S0140-6736(18)31694-5

32. Allel K, Day L, Hamilton A, *et al*. Global antimicrobial-

resistance drivers: An ecological country-level study at the human-animal interface. *Lancet Planet Health*. 2023;7(4):e291-e303.

doi: 10.1016/S2542-5196(23)00026-8

33. Tanimura T, Jaramillo E, Weil D, Raviglione M, Lönnroth K. Financial burden for tuberculosis patients in low-and middle-income countries: A systematic review. *Eur Respir J*. 2014;43(6):1763-1775.

doi: 10.1183/09031936.00193413

34. Phan J, Nair D, Jain S, *et al*. Alterations in gut microbiome composition and function in irritable bowel syndrome and increased probiotic abundance with daily supplementation. *mSystems*. 2021;6(6):e01215-21.

doi: 10.1128/mSystems.01215-21

35. De Gaetano GV, Lentini G, Famà A, Coppolino F, Beninati C. Antimicrobial resistance: Two-component regulatory systems and multidrug efflux pumps. *Antibiotics* (*Basel*). 2023;12(6):965.

doi: 10.3390/antibiotics12060965

36. Alock BP, Raphenya AR, Lau TTY, *et al*. CARD 2020: Antibiotic resistome surveillance with the comprehensive antibiotic resistance database. *Nucleic Acids Res*. 2020;48:D517-D525.

doi: 10.1093/nar/gkz935

37. Barbour A, Smith L, Oveisi M, *et al*. Discovery of phosphorylated lantibiotics with proimmune activity that regulate the oral microbiome. *Proc Natl Acad Sci U S A*. 2023;120(22):e2219392120.

doi: 10.1073/pnas.2219392120

38. Pei ZF, Zhu L, Sarksian R, van der Donk WA, Nair SK. Class V Lanthipeptide cyclase directs the biosynthesis of a stapled peptide natural product. *J Am Chem Soc*. 2022;144(38):17549-17557.

doi: 10.1021/jacs.2c06808

39. Tovillas P, Navo CD, Oroz P, *et al*. Synthesis of β2,2-amino acids by stereoselective alkylation of isoserine derivatives followed by nucleophilic ring opening of quaternary sulfamidates. *J Org Chem*. 2022;87(13):8730-8743.

doi: 10.1021/acs.joc.2c01034

40. Bothwell IR, Caetano T, Sarksian R, Mendo S, van der Donk WA. Structural analysis of class I Lanthipeptides from *Pedobacter lusitanus* NL19 reveals an unusual ring pattern. *ACS Chem Biol*. 2021;16(6):1019-1029.

doi: 10.1021/acschembio.1c00106

41. Joaquin D, Lee MA, Kastner DW, *et al*. Impact of dehydroamino acids on the structure and stability of incipient 3_{10}-helical peptides. *J Org Chem*. 2020;85(3):1601-1613.

doi: 10.1021/acs.joc.9b02747

42. De Luca S, Digilio G, Verdoliva V, Tovillas P, Jiménez-Osés G, Peregrina JM. Lanthionine peptides by S-alkylation with substituted cyclic sulfamidates promoted by activated molecular sieves: Effects of the sulfamidate structure on the yield. *J Org Chem*. 2019;84(22):14957-14964.

doi: 10.1021/acs.joc.9b02306

43. Dickman R, Mitchell SA, Figueiredo AM, Hansen DF, Tabor AB. Molecular recognition of lipid II by Lantibiotics: Synthesis and conformational studies of analogues of nisin and mutacin rings A and B. *J Org Chem*. 2019;84(18):11493-11512.

doi: 10.1021/acs.joc.9b01253

44. Chen H, Zhang Y, Li QQ, Zhao YF, Chen YX, Li YM. De novo design to synthesize lanthipeptides involving cascade cysteine reactions: SapB Synthesis as an example. *J Org Chem*. 2018;83(14):7528-7533.

doi: 10.1021/acs.joc.8b00259

45. Ma C, Peng Y, Li H, Chen W. Organ-on-a-Chip: A new paradigm for drug development. *Trends Pharmacol Sci*. 2021;42(2):119-133.

doi: 10.1016/j.tips.2020.11.009

46. Najmi A, Javed SA, Al Bratty M, Alhazmi HA. Modern approaches in the discovery and development of plant-based natural products and their analogues as potential therapeutic agents. *Molecules*. 2022;27(2):349.

doi: 10.3390/molecules27020349

47. Sivadas N, Kaul G, Akhir A, *et al*. Naturally derived malabaricone B as a promising bactericidal candidate targeting multidrug-resistant *Staphylococcus aureus* also possess synergistic interactions with clinical antibiotics. *Antibiotics* (*Basel*). 2023;12(10):1483.

doi: 10.3390/antibiotics12101483

48. Torres MT, de la Fuente-Nunez C. Toward computer-made artificial antibiotics. *Curr Opin Microbiol*. 2019;51:30-38.

doi: 10.1016/j.mib.2019.03.004

49. Torres MDT, Cao J, Franco OL, Lu TK, de la Fuente-Nunez C. Synthetic biology and computer-based frameworks for antimicrobial peptide discovery. *ACS Nano*. 2021;15(2):2143-2164.

doi: 10.1021/acsnano.0c09509

50. Aronica PGA, Reid LM, Desai N, *et al*. Computational methods and tools in antimicrobial peptide research. *J Chem Inf Model*. 2021;61(7):3172-3196.

doi: 10.1021/acs.jcim.1c00175

51. Gray DA, Wenzel M. Multitarget approaches against multiresistant superbugs. *ACS Infect Dis*. 2020;6(6):1346-1365.

doi: 10.1021/acsinfecdis.0c00001

52. Fields FR, Lee SW, McConnell MJ. Using bacterial genomes and essential genes for the development of new antibiotics. *Biochem Pharmacol*. 2017;134:74-86.

doi: 10.1016/j.bcp.2016.12.002

53. Rana R, Awasthi R, Sharma B, Kulkarni GT. Nanoantibiotic formulations to combat antibiotic resistance - old wine in a new bottle. *Recent Pat Drug Deliv Formul*. 2019;13(3):174-183.

doi: 10.2174/1872211313666190911124626

54. Munir MU, Ahmed A, Usman M, Salman S. Recent advances in nanotechnology-aided materials in combating microbial resistance and functioning as antibiotics substitutes. *Int J Nanomedicine*. 2020;15:7329-7358.

doi: 10.2147/IJN.S265934

55. Manrique PD, López CA, Gnanakaran S, Rybenkov VV, Zgurskaya HI. New understanding of multidrug efflux and permeation in antibiotic resistance, persistence, and heteroresistance. *Ann N Y Acad Sci*. 2023;1519(1):46-62.

doi: 10.1111/nyas.14921

56. Mulat M, Pandita A, Khan F. Medicinal plant compounds for combating the multi-drug resistant pathogenic bacteria: A review. *Curr Pharm Biotechnol*. 2019;20(3):183-196.

doi: 10.2174/1872210513666190308133429

57. Tarín-Pelló A, Suay-García B, Pérez-Gracia MT. Antibiotic resistant bacteria: Current situation and treatment options to accelerate the development of a new antimicrobial arsenal. *Expert Rev Anti Infect Ther*. 2022;20(8):1095-1108.

doi: 10.1080/14787210.2022.2078308

58. Lv S, Wang Y, Jiang K, *et al*. Genetic engineering and biosynthesis technology: Keys to unlocking the chains of phage therapy. *Viruses*. 2023;15(8):1736.

doi: 10.3390/v15081736

59. Zeituni EM, Raterman EL. NIAID's comprehensive support mechanisms for antibiotic development. *ACS Infect Dis*. 2020;6(6):1299-1301.

doi: 10.1021/acsinfecdis.0c00099

60. Lluka T, Stokes JM. Antibiotic discovery in the artificial intelligence era. *Ann N Y Acad Sci*. 2023;1519(1):74-93.

doi: 10.1111/nyas.14930

61. Xavier BB, Das AJ, Cochrane G, *et al*. Consolidating and exploring antibiotic resistance gene data resources. *J Clin Microbiol*. 2016;54(4):851-859.

doi: 10.1128/JCM.02717-15